Electronic pump regulates Fe-Co catalytic center to enhance advanced oxidation performance

Zhengxi Chen[a], Yujie Cui[a], Liwei Yang[a], Ruoying Wang[a], Xuejun Pan[*c,d], and Fengzhi Jiang[*a,b]

a. School of Chemical Science and Technology, Yunnan University, Kunming, 650500, China.

b. Institute of International Rivers and Eco-Security, Yunnan University, Kunming, 650500, China.

c. Southwest United Graduate School, Kunming, 650092, China.

d. Faculty of Environmental Sciences and Engineering, Kunming University of Science and Technology, Kunming, 650500, China.

* Corresponding author.

E-mail: fengzhij@ynu.edu.cn，xjpan@kust.edu.cn

Experimental method

Experimental reagents: The reagents used in this experiment were of analytical grade (AR). The specific sources and information are as follows: ferric chloride hexahydrate ($FeCl_3 \cdot 6H_2O$), 2-aminoterephthalic acid (NH_2-BDC, molecular formula $C_8H_7NO_4$), cobalt nitrate hexahydrate ($Co(NO_3) \cdot 6H_2O$), hydrochloric acid (HCl) were purchased from Adamas-beta; N,N-dimethylformamide (DMF, molecular formula C_3H_7NO) was provided by Tianjin Zhiyuan ; potassium peroxymonosulfate($KHSO_5$) and humic acid(HA, molecular formula $C_9H_9NO_6$) were purchased from Aladdin. Benzoquinone (p-BQ, molecular formula $C_6H_4O_2$) and furfuryl alcohol (FFA, molecular formula $C_5H_6O_2$) were from Adamas. Sulfamethoxazole (SMX, molecular formula $C_{10}H_{11}N_3O_3S$), tert-butanol (TBA, molecular formula $C_4H_{10}O$), sulfadiazine (SDZ, molecular formula $C_{10}H_{10}N_4O_2S$), sodium hydroxide (NaOH), ciprofloxacin (CIP, molecular formula $C_{17}H_{18}FN_3O_3$), tetracycline hydrochloride (molecular formula $C_{22}H_{25}ClN_2O_8$) were supplied by Sigma-Aldrich. The polytetrafluoroethylene (PTFE) hydrophilic membrane used in the experiment came from sea salt plasticizing technology. All reagents were directly used in the experiment without further purification.

Experimental equipment: The main equipment used in this experiment is as follows: analytical balance (model ML-104, Mettler-Toledo) for accurate weighing of reagents; the magnetic stirrer (model RCT-basic, IKA) is used for the mixing and stirring of the solution; the electrothermal constant temperature drying oven (model 202-OES, Shanghai Yiheng) is used for the constant temperature drying treatment of the sample; desktop low-speed centrifuge (W25K, Beijing median) for solid-liquid separation operation; the ultra-pure water machine (model UPH-3V-10T, Shanghai Youpu) is used to prepare ultra-pure water for the experiment; ultrasonic cleaner (model KQ-500E, Kunshan Shumei) is used for instrument cleaning and sample dispersion; the pH meter (model PHS-25, Shanghai Yidian) is used to determine the pH value of the solution. The contact angle measuring instrument (OCA25, Dataphysics, Germany)

was used to characterize the wettability of the material surface. High performance liquid chromatography (Agilent 1260, Agilent Technologies) for quantitative analysis of target substances; the constant temperature culture shaker (model NSKY-200 B, Shanghai Sukun) is used for the constant temperature shock culture of the sample; inductively coupled plasma emission spectrometer (Optima 8300, PerkinElmer) for the detection and analysis of element content; peristaltic pump (model YZ15, Baoding Frey) is used for precise transportation of fluid. The electrochemical workstation (model CHI760E, Shanghai Chenhua) is used for electrochemical related performance testing.

Characterization techniques: In this study, a variety of characterization techniques were used to comprehensively characterize the crystal structure, surface properties, micromorphology and functional groups of the samples. The crystal structure and phase analysis were carried out by X-ray diffractometer (XRD, Rigaku SmartLab SE). The test conditions were the radiation source Cu target Kα, the scanning rate was 10°/min; the elemental composition and chemical valence state of the sample surface were analyzed by X-ray photoelectron spectroscopy (XPS, Thermo Scientific K-Alpha). The test conditions were Al Kα ray (hv=1486.6 eV), working voltage 12 kV, filament current 6 mA; the microstructure of the sample was observed by scanning electron microscopy (SEM, Hitachi Regulus 8100), and the material was adhered to the conductive adhesive during sample preparation. The microstructure analysis was carried out by transmission electron microscopy (TEM，JEOL JEM·2100F). The material was first dispersed in ethanol, and then added to the micro-grid copper mesh. The BET (Quantachrome Nova 4000e) was used to analyze the specific surface area, pore and pore size of the sample, and the adsorbed gas was N_2; the surface wettability of the material was characterized by a contact angle measuring instrument (DataPhysics). Fourier transform infrared spectroscopy (FT-IR, Bruker Tensor·27) was used to identify the functional groups of the samples. During the test, the powder was conventionally pressed and the scanning range was 400-4000 cm^{-1}. The types and concentrations of free radicals were detected by electron spin resonance spectrometer

(EPR，Bruker EMXPLUS 6/1). The test conditions were 300 W xenon lamp, and the capture agents were DMPO and TEMP. The leaching concentration of metal ions was determined by inductively coupled plasma technology (ICP, Agilent 7700s). The solution to be tested needs to pass a 0.45μm filter before testing.

Preparation of MIL-101(Fe)-NH_2 catalyst: 2.027 g $FeCl_3 \cdot 6H_2O$ and 1.2 mL acetic acid were dissolved in 85 mL DMF and dispersed in an ultrasonic cleaner for 5 min to obtain a homogeneous precursor solution. 4 mmol NH_2-BDC was added and magnetically stirred at room temperature for 30 min. The mixed solution was transferred to a 200 mL PTFE-lined high-pressure reactor and reacted at 130 °C for 48 h. After the reaction, the solid was centrifuged, washed three times with methanol and deionized water, and vacuum dried at 60 °C overnight to obtain MIL-101(Fe)-NH_2.

Preparation of MIL-101(CoFe)-NH_2 catalyst and samples with different Fe:Co precursor feeding ratios: MIL-101 (Fe)-NH_2 was used as the control material, and FeCo bimetallic MIL-101(CoFe)-NH_2 was constructed by solvothermal one-step introduction of Co. 1.014 g $FeCl_3 \cdot 6H_2O$, 1.091 g $Co(NO_3)_2 \cdot 6H_2O$ and 1.2 mL acetic acid were added into 85 mL N,N-dimethylformamide (DMF) and dispersed in an ultrasonic cleaner for 5 min to obtain a homogeneous precursor solution. Subsequently, 4 mmol NH_2-BDC was added and magnetically stirred at room temperature for 30 min. The mixed solution was transferred to a 200 mL polytetrafluoroethylene autoclave and reacted at 130 °C for 48 h. After the reaction, the solid was centrifuged, washed three times with methanol and deionized water, and dried in vacuum at 60 °C overnight to obtain MIL-101(CoFe)-NH_2 sample.

To evaluate the effect of Co incorporation, MIL-101(CoFe)-NH_2 samples with different Fe:Co precursor feeding ratios were further prepared using the same solvothermal procedure while keeping the total molar amount of metal precursors constant. In addition to the Fe:Co = 1:1 sample described above, samples with Fe:Co precursor feeding ratios of 2:1 and 1:2 were prepared. For the Fe:Co = 2:1 sample, 1.352 g $FeCl_3 \cdot 6H_2O$ and 0.728 g $Co(NO_3)_2 \cdot 6H_2O$ were used; for the Fe:Co = 1:2

sample, 0.676 g $FeCl_3 \cdot 6H_2O$ and 1.455 g $Co(NO_3)_2 \cdot 6H_2O$ were used. Other synthetic conditions, including the amounts of NH_2-BDC, acetic acid and DMF, reaction temperature, reaction time, washing, and drying procedures, were kept identical. Unless otherwise specified, MIL-101(CoFe)-NH_2 in this work refers to the sample prepared with the Fe:Co precursor feeding ratio of 1:1.

ICP-OES analysis was used to determine the actual Fe and Co contents of the samples. Before measurement, 10 mg of catalyst was digested in 5 mL aqua regia and then diluted to 10 mL with deionized water. For the samples prepared with Fe:Co precursor feeding ratios of 2:1, 1:1, and 1:2, the measured Co contents were 0.45, 1.54, and 3.71 wt%, respectively, while the corresponding Fe contents were 15.34, 18.05, and 14.29 wt%, respectively. These results show that the actual Co incorporation was lower than the nominal precursor feeding ratio but increased with increasing Co precursor dosage. For the optimized Fe:Co = 1:1 sample, the actual Fe:Co atomic ratio was approximately 12:1, indicating limited but effective Co incorporation into the Fe-based MIL-101 framework.

Preparation of MIL-101(CoFe)-NH_2/PTFE catalytic membrane: PTFE microporous membrane (pore size: 0.45 μm) with a diameter of 47 mm was immersed in ethanol and water for 1 h to remove surface impurities, and then dried at 60 °C overnight. 0.1 g MIL-101(CoFe)-NH_2 catalyst material was dissolved in 100 mL deionized water and ultrasonically dispersed to uniform. The washed PTFE membrane was placed on the sand core of the sand filter funnel, and the upper suction filter bottle was fixed. The vacuum pump was opened, and the MIL-101(CoFe)-NH_2 solution was poured into the upper suction filter bottle. The catalyst material was vacuum filtered to all load on the PTFE filter membrane, dried overnight at 60 °C to prepare a catalytic membrane, which was recorded as MIL-101(CoFe)-NH_2/PTFE membrane.

Catalytic performance test: In this study, 10 mg/L SDZ was used as the target pollutant, and the degradation performance of the catalytic material was tested at room temperature (25 ± 2 °C). During the experiment, 50 mL of SDZ solution with an initial

concentration of 10 mg/L was mixed with a certain amount of catalyst material and an appropriate amount of PMS solution, and then placed in a constant temperature oscillator for 10 min to start the reaction. During the reaction, 2 mL of the reaction solution was taken at intervals, filtered using a glass fiber filter membrane, and the residue in the reaction solution was determined by HPLC. In order to evaluate the broad-spectrum applicability of catalytic materials, CIP, OTC, TC and SMX with the same initial concentration of 10 mg/L were further selected as representative antibiotic pollutants, and degradation experiments were carried out according to the same method to verify the material 's ability to treat a variety of organic pollutants. The removal efficiency of SDZ by catalyst materials was calculated by the following formula:

$$R=(C_0-C)/C_0\times 100\ \%$$

In the formula, R is the removal efficiency of SDZ (%), C_0 and C are the initial concentration of SDZ and the concentration after a certain time of reaction, respectively.

The data of SDZ degradation experiment by activated PMS were fitted by quasi-first-order kinetic reaction rate equation. The equation used was:

$$ln(C/C_0) =-kt$$

In the formula, k is the rate constant of the catalytic reaction, and t is the reaction time.

PMS consumption rate: The residual PMS concentration was determined by the iodometric method. Briefly, aliquots were collected at predetermined reaction intervals and immediately filtered to remove the catalyst. The filtered solution was then mixed with excess potassium iodide under acidic conditions, during which the residual PMS oxidized I^- to I_3^-. The generated I_3^- was quantified by UV-vis spectroscopy according to a standard calibration curve. The PMS utilization efficiency was calculated as follows:

$$PMS\ utilization\ (\%) =(C_0-C_t)/C_0\times 100\ \%$$

where C_0 and C_t are the initial PMS concentration and residual PMS concentration at reaction time t, respectively.

Catalyst stability test: The stability of MIL-101(CoFe)-NH_2 was investigated by cyclic catalytic experiments. The catalyst was recovered after each round of reaction, and then used for PMS activation and degradation of SDZ after ethanol dispersion, centrifugal washing and drying to evaluate its recycling performance.

Determination of pollutant concentration: The concentration of SDZ, CIP, OTC and TC pollutants was determined by high performance liquid chromatography. The specific method was as follows: SDZ: the column temperature was 30.0 ℃, the elution condition was the flow rate of 1 mL/min, acetonitrile and water containing 0.1% formic acid were mixed at a ratio of 30:70; CIP: The chromatographic column temperature was 30.0 ℃, the elution condition was the flow rate was 1 mL/min, acetonitrile and water containing 0.1% formic acid were mixed at a ratio of 20:80; TC: The chromatographic column temperature was 30.0 ℃, the elution condition was the flow rate was 0.8 mL/min, methanol and water containing 0.1% formic acid were mixed at a ratio of 50:50; OTC: The column temperature was 30.0 ℃. the elution condition was the flow rate was 0.8 mL/ min, acetonitrile and water containing 0.1 % formic acid were mixed at a ratio of 30:70.

Electrochemical measurements: The i-t chronoamperometry measurements were performed on an electrochemical workstation using a conventional three-electrode system. A glassy carbon electrode was used as the working electrode, a saturated calomel electrode was used as the reference electrode, and a platinum electrode was used as the counter electrode. PBS buffer solution was used as the electrolyte. The applied potential was set at 0.45 V, the sampling interval was 0.1 s, and the total running time was 220 s.

PMSO probe experiment for high-valent metal species: The possible contribution of high-valent metal-oxo species was evaluated using methyl phenyl sulfoxide (PMSO) as a probe molecule. Typically, 50 mL of PMSO solution was mixed with 6 mg of MIL-101(CoFe)-NH_2 and 0.1 mM PMS under the same reaction conditions as the SDZ degradation experiment. The reaction was carried out at room temperature under continuous shaking. At predetermined time intervals, aliquots were withdrawn and immediately filtered through a 0.45 μm membrane to remove the catalyst. The concentrations of PMSO and its oxidation product methyl phenyl sulfone ($PMSO_2$)

were analyzed by HPLC. The formation of $PMSO_2$ was used as an indicator for the possible involvement of high-valent metal-oxo species, because PMSO can be selectively oxidized to $PMSO_2$ through oxygen-atom transfer from high-valent metal species. Control experiments without PMS or without catalyst were also conducted for comparison.

DFT calculation method: In this work, all spin-polarized density functional theory calculations are performed using the plane wave code QUANTUM ESPRESSO to complete[1-3]. The exchange correlation potential is approximated by the Perdew-Burke-Ernzerhof functional. The interaction between the core electron and the valence electron is treated by the projection augmented wave method for[4, 5]. The kinetic energy cutoffs of the wave function and the charge density are set to 50 Ry and 500 Ry, respectively. The convergence criteria of the force on each atom in the process of electronic structure iteration and structural relaxation are set to 10^{-8} Ry and 5×10^{-4} Ry/Bohr, respectively. The model uses MIL-101(Fe)-NH_2 and MIL-101(CoFe)-NH_2 units, and a vacuum layer of 15 Å is set up to avoid the interaction between periodic images. In the geometric optimization process, the Brillouin zone sampling uses a 2×2×1 Γ-center Monkhorst-Pack k point grid. Gaussian broadening with a width of 10^{-3} Ry is used to accelerate the convergence of the electronic structure. In all calculations, the van der Waals interaction is described by the DFT-D3 method in the Grimme scheme[6]. The PBE functional was selected as a practical balance between computational cost and accuracy for the relatively large periodic MOF system. Although PBE may underestimate band gaps and some adsorption energies, it generally provides reliable optimized geometries and reasonable relative energetics for MOF systems when combined with appropriate dispersion corrections. Grimme's DFT-D3 correction was explicitly included to account for Van der Waals interactions, which are important for describing the flexible pore environment and PMS–framework interactions in MIL-type MOFs.

Performance test of SDZ degradation by catalytic membrane system: The device of SDZ degradation by catalytic membrane system is shown in Fig. S12, which is composed of peristaltic pump, feed liquid, filtrate, catalytic membrane and fixed membrane reactor. The 10 mg/L SDZ solution was used as the feed solution, and a certain concentration of PMS was added and stirred evenly to obtain the feed solution.

The prepared catalytic membrane was placed in a fixed membrane reactor. At a certain flow rate, the pressure of the peristaltic pump was used to make the feed liquid pass through the catalytic membrane and flow into the beaker below to obtain the filtrate after the reaction, and the filtrate was no longer returned to the feed liquid. The filtrate was collected at a certain time interval and the concentration of SDZ was measured by HPLC.

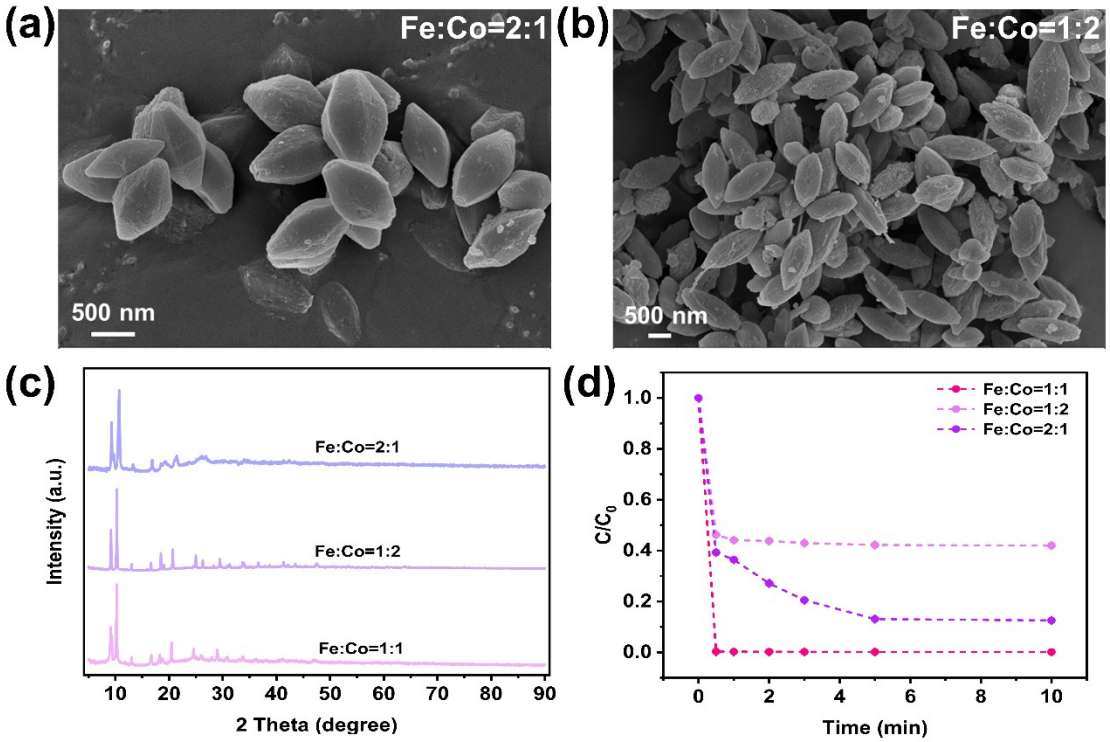

Fig. S1 SEM images of MIL-101(CoFe)-NH_2 prepared with Fe:Co precursor feeding ratios of 2:1 (a) and 1:2 (b); XRD patterns (c) and degradation performance (d) of MIL-101(CoFe)-NH_2 samples prepared with different Fe:Co precursor feeding ratios

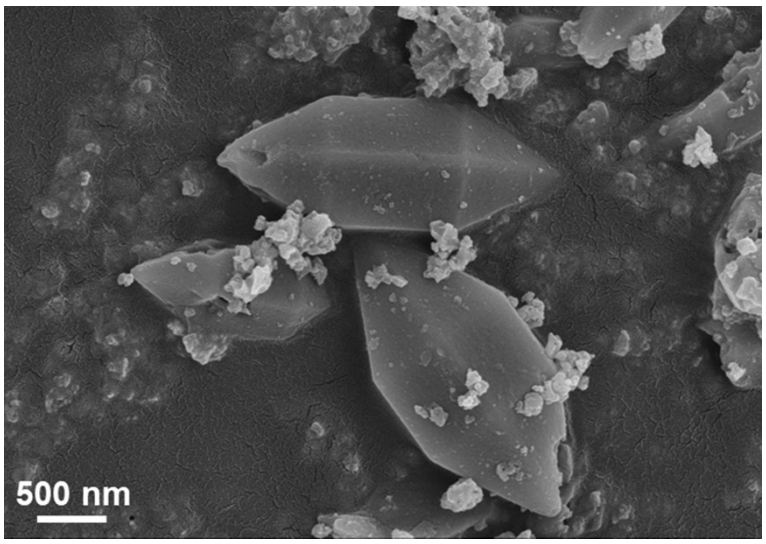

Fig. S2 SEM image of MIL-101(Fe)-NH_2

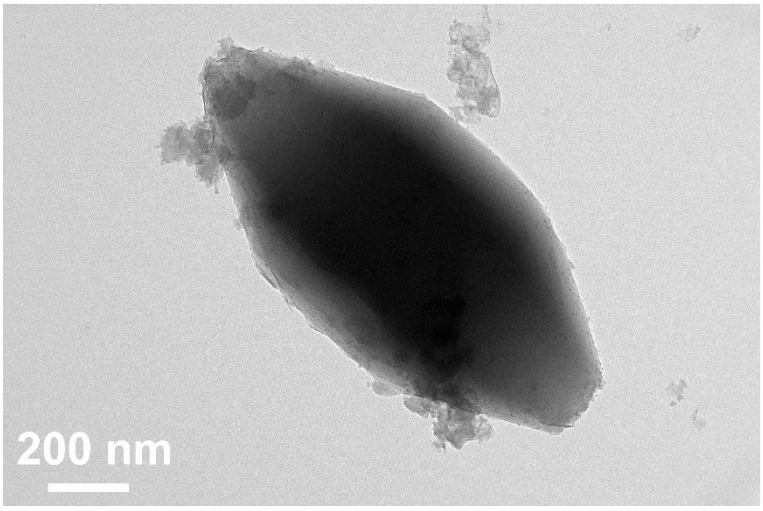

Fig. S3 TEM image of MIL-101(CoFe)-NH_2

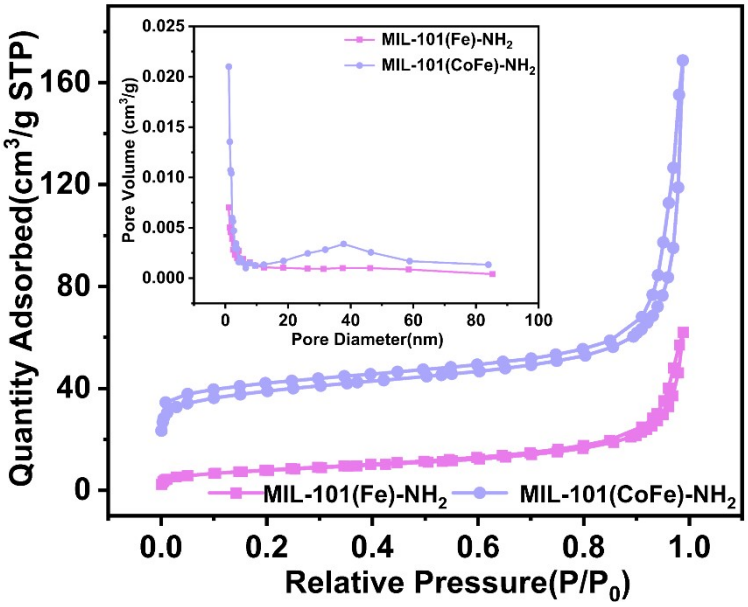

Fig. S4 BET diagrams of MIL-101(Fe)-NH_2 and MIL-101(CoFe)-NH_2 materials

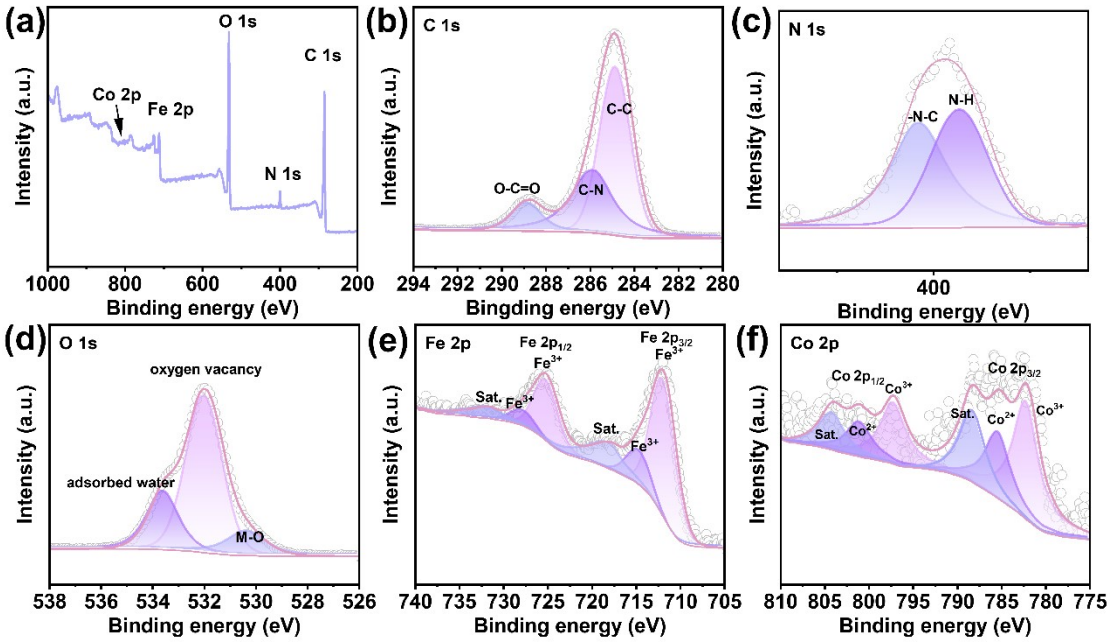

Fig. S5 XPS spectra of MIL-101(CoFe)-NH_2: survey spectrum (a), C 1s (b), N 1s (c), O 1s (d), Fe 2p (e) and Co 2p (f)

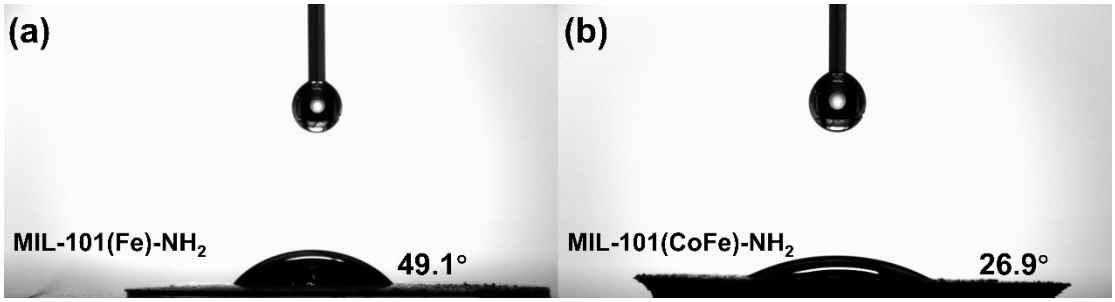

Fig. S6 Contact angles of MIL-101(Fe)-NH_2 (a) and MIL-101(CoFe)-NH_2 (b)

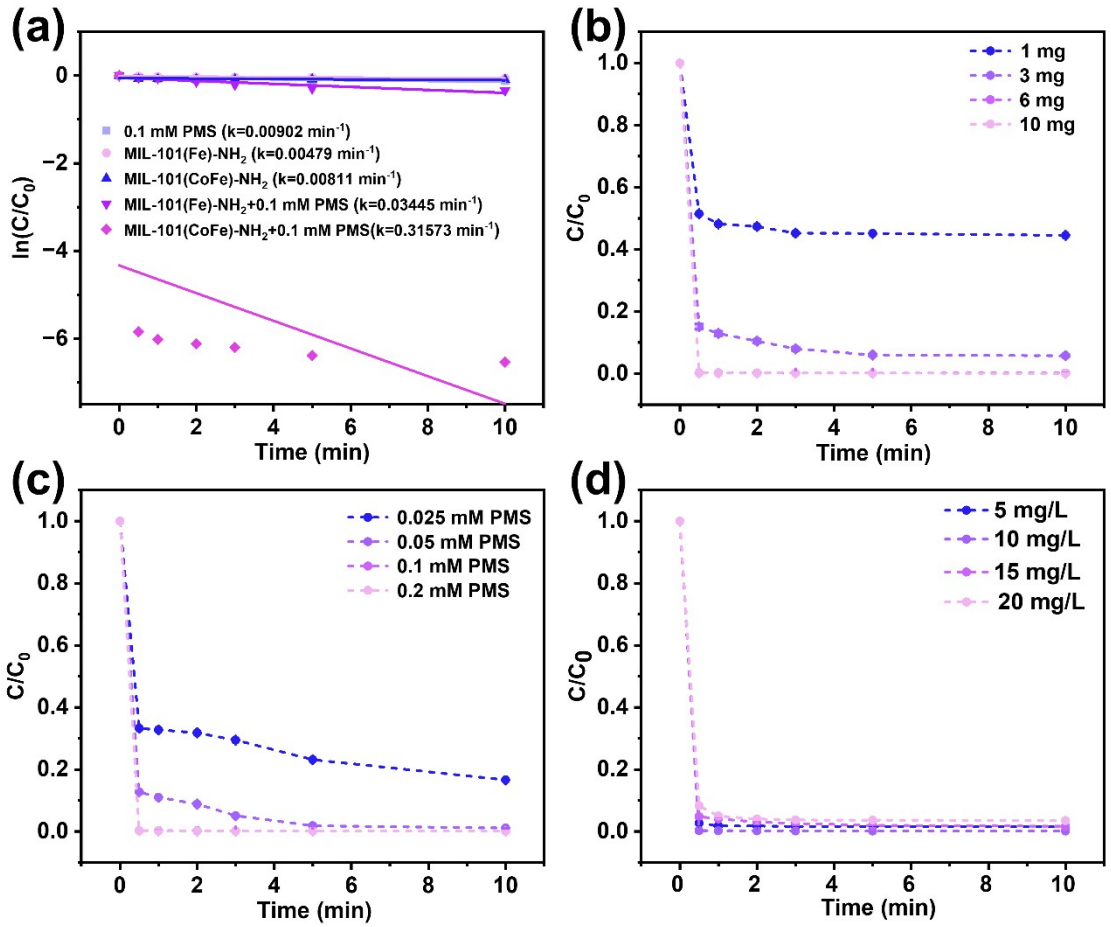

Fig. S7 Pseudo-first-order kinetic fitting plots of degradation performance of various catalysts (a); Effects of different conditions on the degradation of SDZ by MIL-101(CoFe)-NH_2: catalyst dosage (b), PMS dosage (c), and pollutant concentration (d)

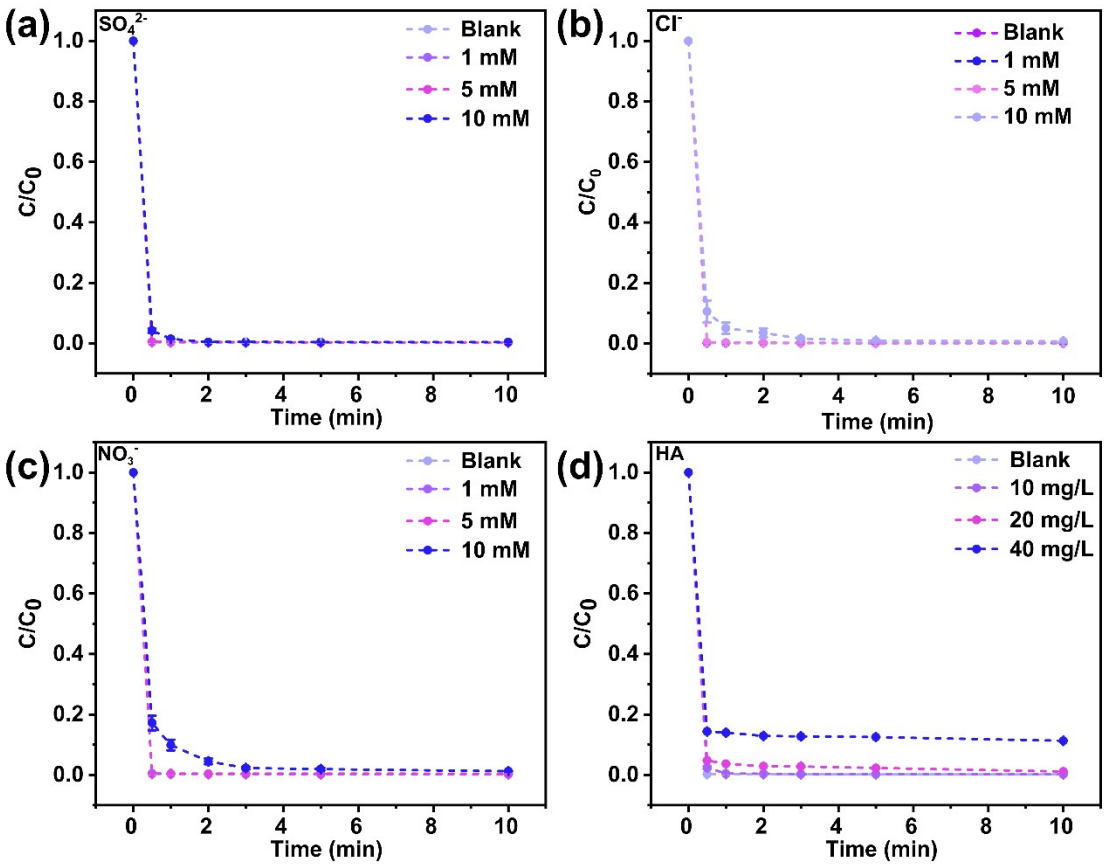

Fig. S8 Effect of coexisting ions and humic acid on the degradation of SDZ by MIL-101(CoFe)-NH_2: SO_4^{2-} (a), Cl^- (b), NO_3^- (c) and HA (d)

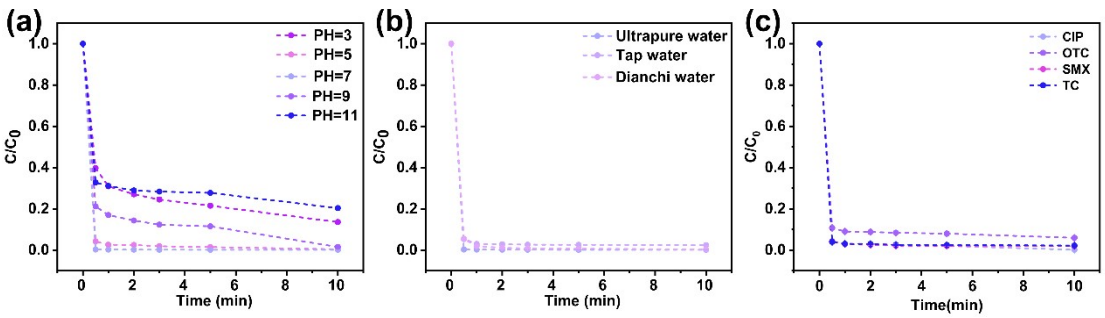

Fig. S9 Effect of different pH (a) and different experimental water bodies (b) on the degradation of SDZ by MIL-101(CoFe)-NH_2; Removal ability of MIL-101(CoFe)-NH_2 catalyst for different antibiotics (c)

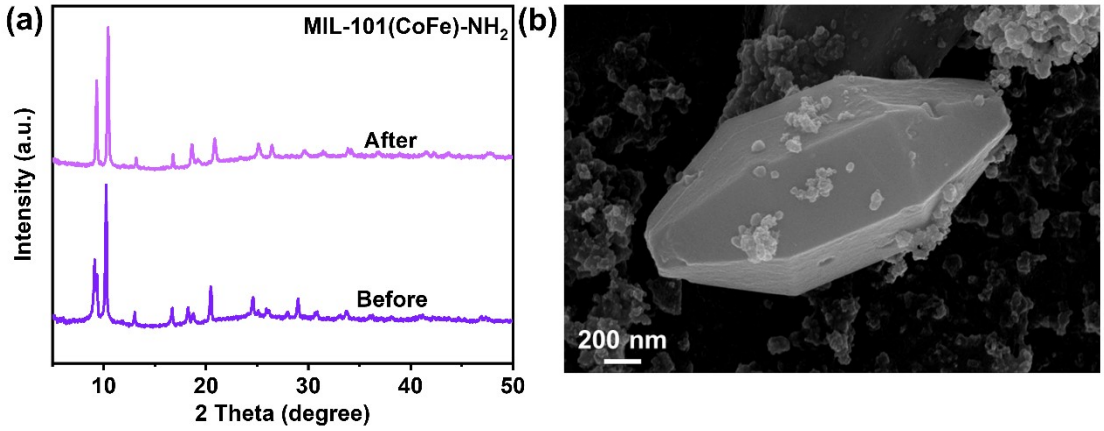

Fig. S10 XRD and SEM of MIL-101(CoFe)-NH_2 after cycling

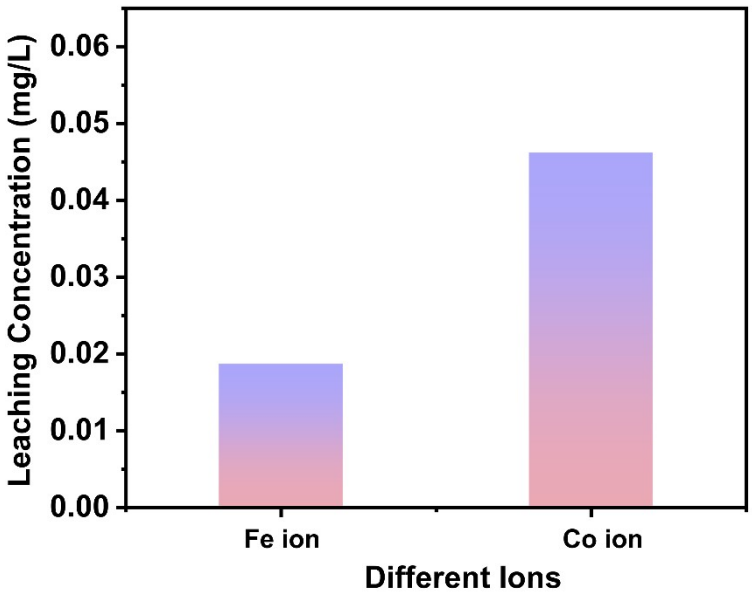

Fig. S11 Leaching concentration of Fe and Co ions

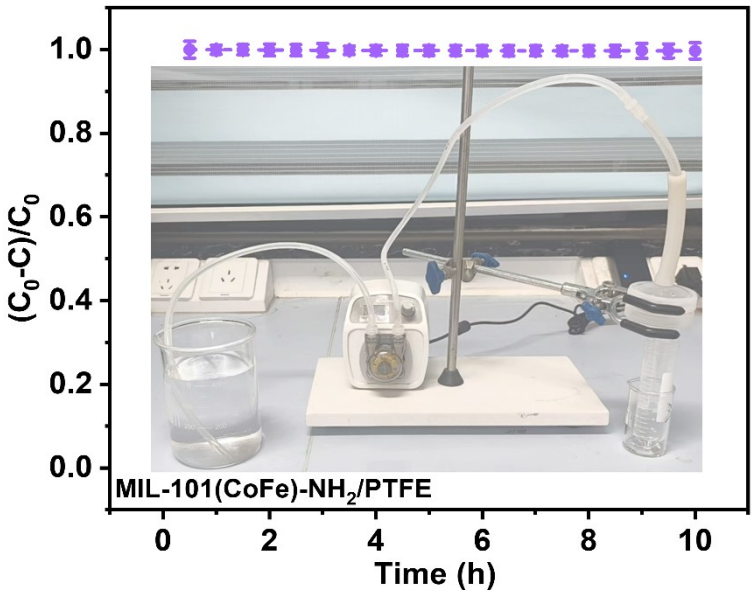

Fig. S12 Continuous flow degradation diagram of MIL-101(CoFe)-NH_2/PTFE membrane

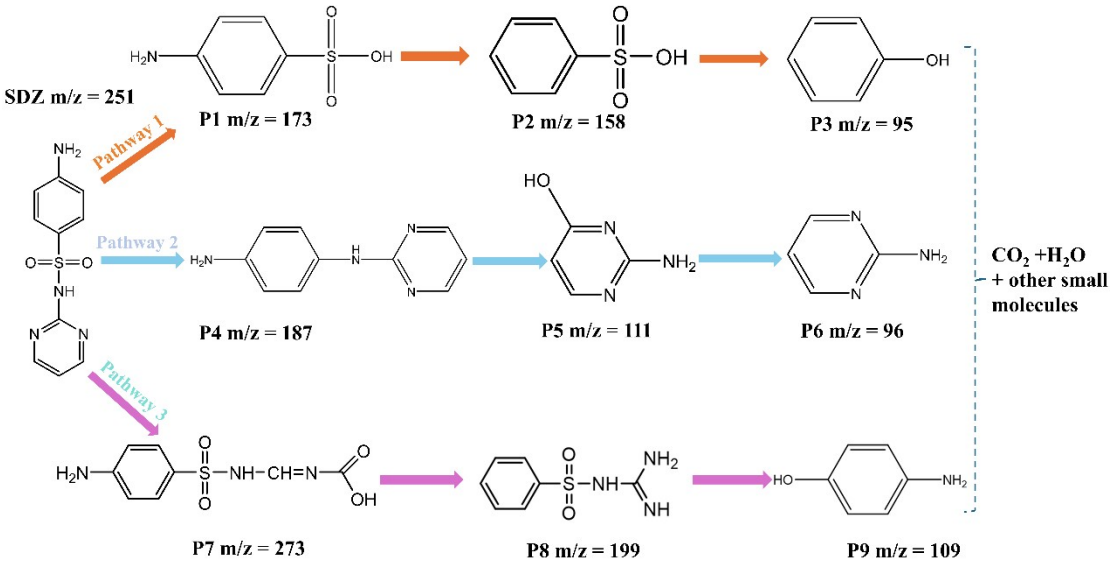

Fig. S13 Possible reaction pathways of SDZ degradation in the MIL-101(CoFe)-NH_2/PMS system

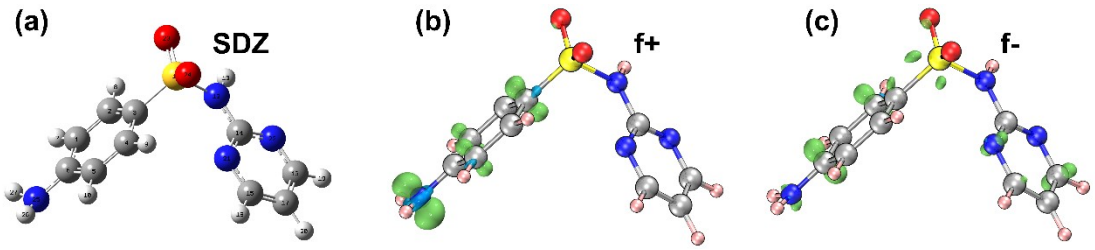

Fig. S14 SDZ molecular structure (a), SDZ Fukui function (f^+) (b) and SDZ Fukui function (f^-) (c) in the MIL-101(CoFe)-NH_2/PMS system

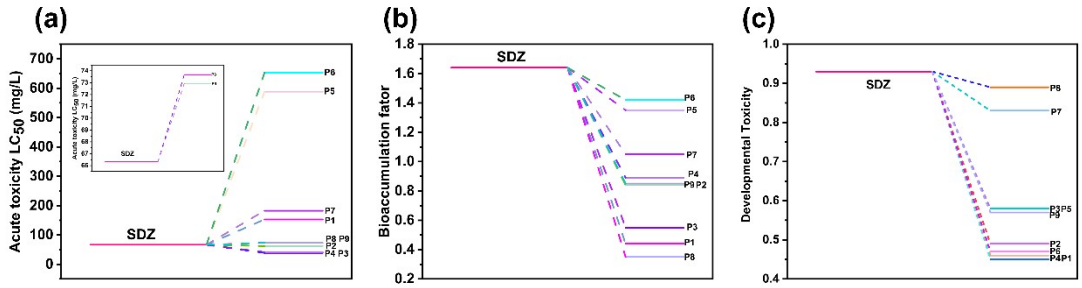

Fig. S15 Acute toxicity (a), bioaccumulation factor (b), and developmental toxicity (c) of different degradation products

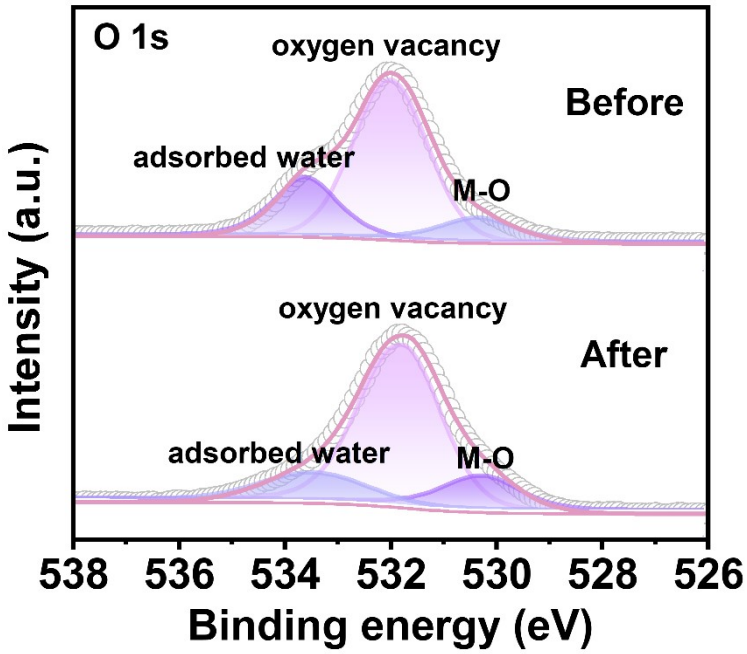

Fig. S16 XPS spectra of O 1s for MIL-101(CoFe)-NH_2 before and after the reaction

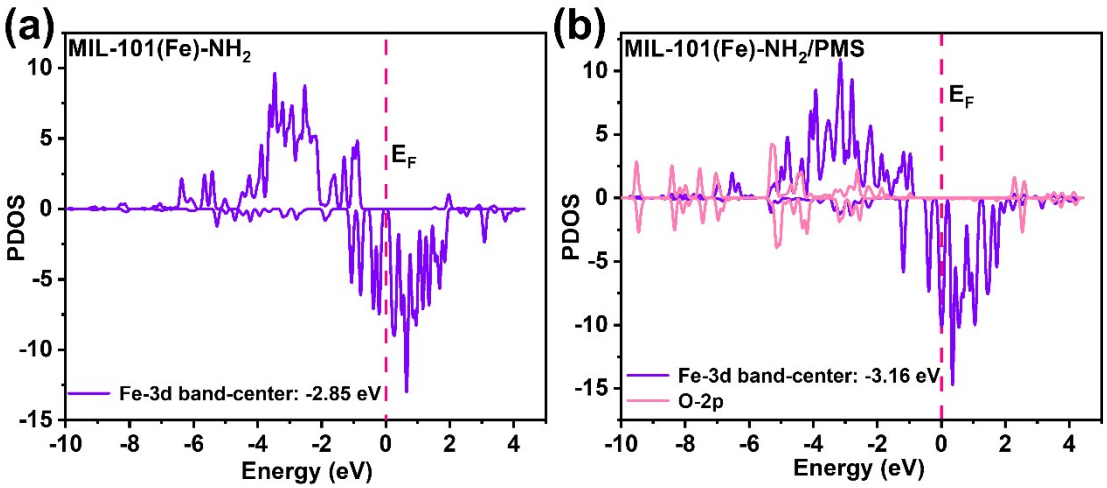

Fig. S17 The density of states of MIL-101(Fe)-NH_2 and the adsorbed PMS

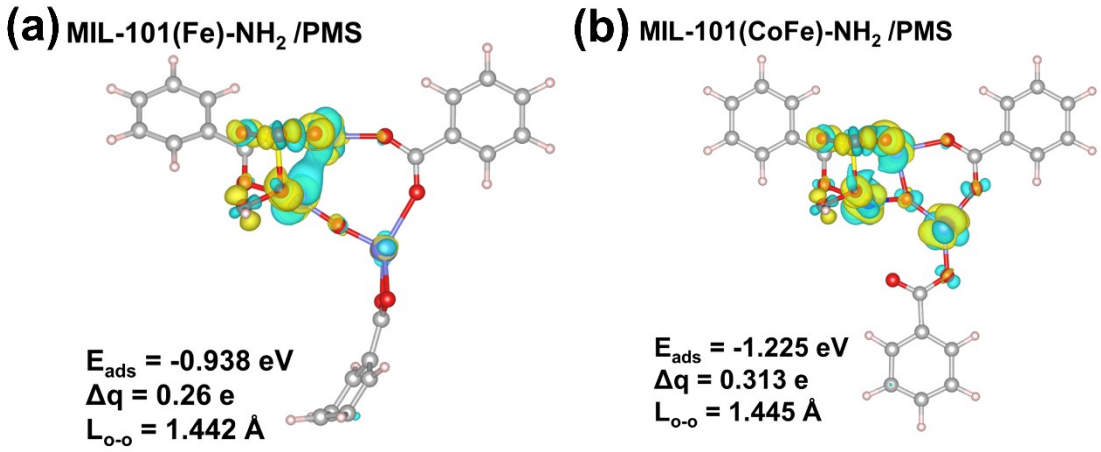

Fig. S18 The differential charge density of adsorbed PMS

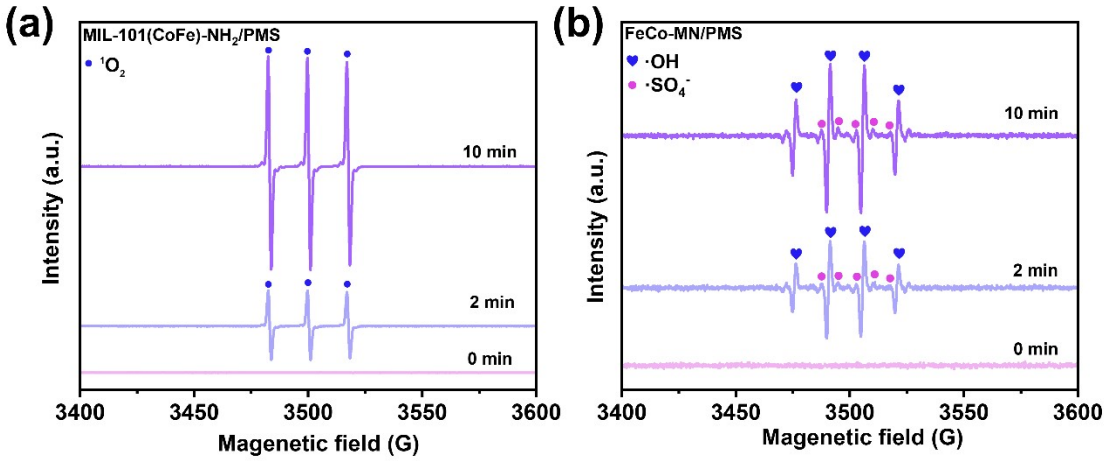

Fig. S19 TEMP-$^1O_2$ test (a) and DMPO-·OH and $\cdot SO_4^-$ tests (b) of MIL-101(CoFe)-NH_2

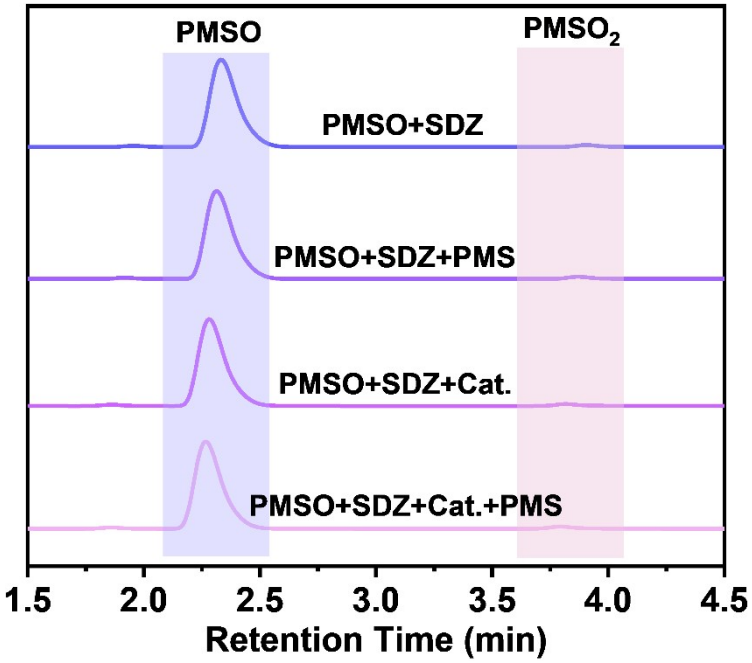

Fig. S20 PMSO-high-valent metal species test of MIL-101(CoFe)-NH_2

References

1. P. Giannozzi, S. Baroni, N. Bonini, M. Calandra, R. Car, C. Cavazzoni, D. Ceresoli, G. L. Chiarotti, M. Cococcioni, I. Dabo, A. Dal Corso, S. de Gironcoli, S. Fabris, G. Fratesi, R. Gebauer, U. Gerstmann, C. Gougoussis, A. Kokalj, M. Lazzeri, L. Martin-Samos, N. Marzari, F. Mauri, R. Mazzarello, S. Paolini, A. Pasquarello, L. Paulatto, C. Sbraccia, S. Scandolo, G. Sclauzero, A. P. Seitsonen, A. Smogunov, P. Umari and R. M. Wentzcovitch, Journal of Physics: Condensed Matter, 2009, 21, 395502.
2. P. Giannozzi, O. Andreussi, T. Brumme, O. Bunau, M. Buongiorno Nardelli, M. Calandra, R. Car, C. Cavazzoni, D. Ceresoli, M. Cococcioni, N. Colonna, I. Carnimeo, A. Dal Corso, S. de Gironcoli, P. Delugas, R. A. DiStasio, A. Ferretti, A. Floris, G. Fratesi, G. Fugallo, R. Gebauer, U. Gerstmann, F. Giustino, T. Gorni, J. Jia, M. Kawamura, H. Y. Ko, A. Kokalj, E. Küçükbenli, M. Lazzeri, M. Marsili, N. Marzari, F. Mauri, N. L. Nguyen, H. V. Nguyen, A. Otero-de-la-Roza, L. Paulatto, S. Poncé, D. Rocca, R. Sabatini, B. Santra, M. Schlipf, A. P. Seitsonen, A. Smogunov, I. Timrov, T. Thonhauser, P. Umari, N. Vast, X. Wu and S. Baroni, Journal of Physics: Condensed Matter, 2017, 29, 465901.
3. P. Giannozzi, O. Baseggio, P. Bonfà, D. Brunato, R. Car, I. Carnimeo, C. Cavazzoni, S. de Gironcoli, P. Delugas, F. Ferrari Ruffino, A. Ferretti, N. Marzari, I. Timrov, A. Urru and S. Baroni, The Journal of Chemical Physics, 2020, 152, 154105.
4. J. Klimeš, D. R. Bowler and A. Michaelides, Physical Review B, 2011, 83, 195131.
5. P. E. Blöchl, Physical Review B, 1994, 50, 17953-17979.
6. S. Grimme, Journal of Computational Chemistry, 2006, 27, 1787-1799.